# Central Lancashire Online Knowledge (CLoK)

| Title | Effect of Layered Double Hydroxide, Expanded Graphite and Ammonium Polyphosphate additives on thermal stability and fire performance of polyisocyanurate insulation foam |
|---|---|
| Type | Article |
| URL | https://clok.uclan.ac.uk/id/eprint/34618/ |
| DOI | https://doi.org/10.1016/j.tca.2020.178724 |
| Date | 2020 |
| Citation | Asimakopoulou, Eleni, Zhang, Jianping, McKee, Maurice, Wieczorek, Kinga, Krawczyk, Anna, Andolfo, Michele, Kozlecki, Tomasz, Scatto, Marco, Sisani, Michele et al (2020) Effect of Layered Double Hydroxide, Expanded Graphite and Ammonium Polyphosphate additives on thermal stability and fire performance of polyisocyanurate insulation foam. Thermochimica Acta, 693. ISSN 0040-6031 |
| Creators | Asimakopoulou, Eleni, Zhang, Jianping, McKee, Maurice, Wieczorek, Kinga, Krawczyk, Anna, Andolfo, Michele, Kozlecki, Tomasz, Scatto, Marco, Sisani, Michele, Bastianini, Maria, Karakassides, Anastasios and Papakonstantinou, Pagona |

# Journal Pre-proof

Effect of Layered Double Hydroxide, Expanded Graphite and Ammonium Polyphosphate additives on thermal stability and fire performance of polyisocyanurate insulation foam

Eleni Asimakopoulou (Conceptualization) (Methodology) (Investigation) (Formal analysis) (Validation) (Writing - original draft), Jianping Zhang (Conceptualization) (Methodology) (Validation) (Writing - review and editing), Maurice Mckee (Investigation), Kinga Wieczorek (Resources) (Methodology), Anna Krawczyk (Resources) (Methodology) (Validation)<ce:contributor-role>Wirting - review and editing), Michele Andolfo (Resources) (Methodology), Tomasz Kozlecki (Resources) (Methodology) (Validation)<ce:contributor-role>Wirting - review and editing), Marco Scatto (Resources) (Methodology), Michele Sisani (Resources) (Methodology), Maria Bastianini (Resources) (Methodology), Anastasios Karakassides (Methodology) (Validation)<ce:contributor-role>Wirting - review and editing), Pagona Papakonstantinou (Methodology) (Validation)<ce:contributor-role>Wirting - review and editing)

Please cite this article as: Asimakopoulou E, Zhang J, Mckee M, Wieczorek K, Krawczyk A, Andolfo M, Kozlecki T, Scatto M, Sisani M, Bastianini M, Karakassides A, Papakonstantinou P,

Effect of Layered Double Hydroxide, Expanded Graphite and Ammonium Polyphosphate additives on thermal stability and fire performance of polyisocyanurate insulation foam, *Thermochimica Acta* (2020), doi: https://doi.org/10.1016/j.tca.2020.178724

# Effect of Layered Double Hydroxide, Expanded Graphite and Ammonium Polyphosphate additives on thermal stability and fire performance of polyisocyanurate insulation foam

Eleni ASIMAKOPOULOU [1], Jianping ZHANG [2], Maurice McKEE [2], Kinga WIECZOREK [3], Anna KRAWCZYK [3], Michele ANDOLFO [3], Marco SCATTO [4], Michele SISANI [4], Maria BASTIANINI [4], Anastasios KARAKASSIDES [5] and Pagona PAPAKONSTANTINOU [5]

[1]School of Engineering, University of Central Lancashire, Flyde Rd, Preston, PR1 2HE, United Kingdom

[2]FireSERT, Belfast School of Architecture and the Built Environment, Ulster University, Newtownabbey BT37 0QB, United Kingdom

[3]SELENA Lab, Ul. Polna 14-18, 55011, Siechnice, Poland

[4]Prolabin and Tefarm SRL, Via dell'Acciaio 9, 06134, Perugia, Italy

[5]Engineering Research Institute, School of Engineering, Ulster University, Newtownabbey BT37 0QB, United Kingdom

Highlights

- Thermal stability and fire behaviour of polyisocyanurate insulation foams with smart fillers
- Such fillers are Layered Double Hydroxides, Expandable Graphite and Ammonium Polyphosphate
- Cone calorimeter data showed that fillers addition decreased heat release rate
- Thermogravimetric analysis coupled with FTIR were used to determine different pyrolysis gases
- Post-burning residuals and morphological evaluation supported the beneficial addition of fillers

**Abstract**

This work examines the effect of Layered Double Hydroxides (LDHs), Expandable Graphite (EG) and Ammonium Polyphosphate (APP) on the thermal stability and behaviour under fire conditions of polyisocyanurate (PIR) insulation foams. Virgin materials' and char residues' morphologies were analyzed with a variety of experimental techniques including field emission scanning electron and optical microscopy along with Raman spectroscopy. Thermal stability and burning behaviour were examined using thermogravimetric (TGA) coupled with Fourier Transform Infrared (FTIR) spectrometer and cone calorimeter. TGA results suggested a decrease in degradation temperature upon introduction of fillers in PIR samples. FTIR spectra were used to determine the absorbance intensity of the different pyrolysis gases. Cone calorimeter data analysis established a limited effect on reducing the rate of heat release rate and smoke production with the inclusion of LDHs. However, EG or EG+APP addition, caused a considerable decrease in heat release rate, owing to the increased char strength and the release of non-combustible gases. The positive effect of EG or EG+APP in the fire behaviour of PIR foams was further supported by the morphological evaluation of their residual char samples.

## 1    Introduction

A worldwide roll-out of near-Zero Energy Buildings drives the design of exterior wall systems with the purpose of achieving building sustainability and high energy efficiency. Energy efficient insulation materials usage in building envelopes is identified as the main practice, that can actively contribute towards achieving greenhouse gases emissions targets and energy consumption reductions [1, 2]. Recent advantages in the development of insulation materials have promoted the use of different types of insulations techniques for external walls. Currently, there is a wide range of insulation options comprising of non-combustible, limited combustible or combustible materials. Most commonly used foams, with or without flame retardants, in the family of polymeric insulation materials include extruded and expanded polystyrene, polyurethane foam (PUF) and polyisocyanurate (PIR) [3]. These inherently combustible and highly insulating materials are extensively used in most construction sectors for their high energy performance and cost benefit but should be designed not to compromise their fire safety.

Recent studies on polymeric foams [e.g., 3-5] have established that their thermal decomposition consists of numerous decomposition pathways that mainly depend on their organic compound reactivity. Specifically, PIR consist of diisocyanates or prepolymers that form ring structures, also referred to as isocyanurate rings [6]. From a thermodynamic point of view, PIR materials are thus considered superior to PURs as they are more thermally stable compared to urethane bonds found in PUR foams. The thermal stability of PIR is demonstrated by the fact that they dissociate at higher temperatures at the range of 350 ºC as opposed to 200 ºC observed for urethanes [7]. Therefore, understanding how the use of reactive or additive flame retardants can modify, reduce, delay or even stop their combustion [3-12] is attracting considerable scientific interest.

To further promote sustainable practices in the construction sector, a growing body of study has been lately devoted to examining the potential of substituting popular halogen-based flame retardants with second-generation eco-friendly substitutes. The study of eco-friendly flame retardants such as Layered Double Hydroxides (LDHs) [4, 5], is of great interest as they are found to increase the flame retardancy and thermal stability in polymers by suppressing smoke and reducing the release of volatile compounds [8]. The benefits of using them also derives from the fact that they may act in both gas and solid phases during polymer combustion. Non-flammable

gases, including water and carbon dioxide, that are released during their combustion can further dilute flammable gases, thus reducing endothermic decomposition of metal hydroxides and promote surface charring of polymers.

The use of different binary and ternary LDHs in various polymeric insulating materials has been investigated by numerous authors; those LDHs include ZnAl and MgAl carbonates, MgAl stearate and ZrP with contents, ranging from 0.2% to 6%, [4, 5, 9]. Despite their effectiveness, LDHs up to now have not met commercial success due to the inherent difficulty to uniformly disperse and distribution in polymers, [4]. Whilst so far, most studies [4, 5, 8] were concerned with fire retardancy effects of LDHs on PUF, recent studies [9, 10, 11] investigated the effect of lamellar inorganic [9] and organic LDHs [11] on flame retardancy of PIR. It has been demonstrated that lamellar inorganic LDHs [9] enhanced the fire retardancy of PIR as initial degradation temperature was increased, degradation was decelerated, and significant char formation was observed. Improved char properties and decreased heat release was also observed when increasing filler's content. Organically modified nanoclay LDHs [11] improved flame retardancy and stability of rosin based PIR foam and showed synergistic effect with other flame retardants. During the combustion process, some of the most efficient LDHs proved to be the Expanded Graphite (EG) and Diethyl Ethylphosphonate. The reason was LDHs' promotion of a reinforced char layer that could provide a more effective thermal barrier against heat and oxygen as well as more effective suppression of smoke and flammable gases.

The synergistic effect of LDHs and other flame retardants, such as EG or Ammonium Polyphosphate (APP), were further investigated [11-17] and recent evidence revealed that the fire behavior of PIR [10, 18] and PUR [19, 20] foams can be substantially improved. This was attributed to the fact that, EG is a graphite intercalation compound with a special layered structure, which is found to expand when exposed to heat forming a huge insulation layer that can further enhance PIR fire resistance [11, 21]. EG having a boiling point above 3000 $^{\circ}$C is able to maintain its integrity as it mainly acts in the condensed phase both in terms of smoke suppression and insulation [19]. This insulation char layer is characterized by a "worm-like" appearance which, results from the expansion of $H_2SO_4$ that is intercalated between graphite layers and the release of $CO_2$, $H_2O$ and $SO_2$ gases [22, 23]. APP consists of a high molecular weight polyphosphate chain and it mainly acts in the condensed phase by contributing to increased char formation [19, 21].

Furthermore, studies revealed that APP and EG can further improve char formation due to the synergy of the phosphoric acid with graphite [19, 22].

Despite previous extensive research on the flammability of PIR and PUR foams [4-12, 18-23], few researchers [11, 18] have investigated the interaction of LDHs with nanometric particles and phosphorous based materials in PIR foams and how they affect their flame retardancy. Therefore, this work aims to extend existing work on polymer flammability [4, 5, 6, 7, 9] and specifically, experimentally investigate the thermal stability and fire behavior of PIR foams containing a range of lamellar inorganic smart fillers, namely LDHs, EG and APP. Emphasis is given on the interaction of LDHs with both APP and EG and how their synergy is contributing towards improved PIR foam flame retardancy. Fire properties and thermal stability of the samples were assessed using cone calorimetry and thermogravimetry techniques coupled with FTIR spectrometry. Virgin materials and char residues morphology was analyzed with a variety of experimental techniques including field emission scanning electron and optical microscopy along with Raman spectroscopy. Post-burning and cellular morphology characterization of the residual materials was also conducted using both field emission scanning microscopy and Raman analysis.

## 2    Experimental investigation

### 2.1    Preparation of materials

PIR samples with an isocyanate index (NCO/OH) of 3.0 were produced at SELENA Labs as described in the previous authors' work [9, 10]. Main components of the samples, including the polyol, the catalysts, the stabilizer and blowing agent (methylal), were initially premixed for up to 3 minutes at 1500 rpm. Polyol blend components' viscosity at 25 $^{\circ}$C was measured below 500 mPa·s and below 260 mPa·s for isocyanate. Fillers were then added to the mix of each different sample and all PIR samples were further mixed for 5 min at 2500 rpm. All fillers used, i.e., Layered Double Hydroxides containing $MgAlCO_3$ (LDH), Expanded Graphite (EG) and Ammonium Polyphosphate with high (APP1) and low degree of polymerization (APP2); final formulations were prepared at SELENA Labs. In more details, EG, provided by Asbury Graphite Mills Inc., has a nominal size greater than 75 μm and Carbon content above 80 % w/w, Sulfur above 3 % w/w

and an expansion ratio of 60:1 cc/g. Carbonate form of MgAl LDH, $Mg_4Al_2(OH)_{12}(CO_3)*6H_2O$, was supplied by Prolabin and Tefarm Srl. Due to its layered structure it is easily employed as an active filler able to improve the efficacy of the main PIR formulation. Ammonium Polyphosphate, $NH_4PO_3$ with high degree of polymerisation (APP1), (average degree of polymerisation n>1000), was used in crystal phase II. It is largely insoluble in water and completely insoluble in organic solvents containing 31-32 % w/w Phosphorus and 14-15 % w/w Nitrogen. APP1 was provided by Clariant Produkte GmbH. It is colourless, non-hygroscopic and non-flammable. It is suitable as a non-halogenated flame retardant for polyurethane foams. It is also biodegradable as it breaks down to naturally occurring phosphate and ammonia with decomposition temperature above 275 ℃. It has a high heat stability, however to prevent APP1 from settling, it was stirred into the mixture. Ammonium Polyphosphate, $NH_4PO_3$ with low degree of polymerisation (APP2), n>50, was used in crystal phase I and supplied by Shandong Chenxu New Material Co. Ltd. P2O5 content was above 69 % w/w and Nitrogen above 13 % w/w.

In total, four formulations were examined, and their fire performance was evaluated against plain PIR samples (REF). Research on LDH and APP additives in PIR revealed that their incorporation in polyurethane composites in a range of concentrations from 0.5 % to 8 %, improved their thermal properties flame retardancy resulting in a decreased HRR [9]. Three different concentration of LDH have been studied, namely 2 %, 4 % and 6 % and the research group decided to use 2 % LDH in order to secure both low price and high efficiency-to-price ratio. EG and APP concentrations were chosen according to scientific literature [11, 12, 13, 18, 20], suppliers' recommendations and our research group previous experience [9, 10]. In that respect, three different formulae flame retardants were used: the first set contained $MgAlCO_3$ at 2 % wt (PL), the second one contained additionally 5.1 % wt EG (PLE) and the third set contained 3.6 % wt APP1 (PLEAPP1) or 3.6 % wt APP2 (PLEAPP2) as depicted in Table 1. The physical and mechanical characteristics of all the samples are presented in Table 1, namely, density, average cell diameter, closed cell percentage, thermal conductivity, compressive strength and tensile strength.

## 2.2 Test methods

### 2.2.1 Morphology and cellular structure

Morphological evaluation of PIR foam samples was conducted at 500 μm with the use of optical microscopy. To provide elemental identification, virgin and charred PIR samples cell structure was further investigated using a field emission scanning electron microscopy (FESEM, Hitachi SU 5000) at 15 kV accelerating voltage. Raman characterization was also used to assess the quality and uniformity of residual chars using an excitation wavelength of 532 nm (RL532C laser source) at a Renishaw Invia Qontor system.

### 2.2.2 TGA - FTIR

Thermogravimetric analysis (TGA) was performed on a Mettler Toledo instrument under both reactive (air) and inert ($N_2$) atmosphere from 20 °C to 700 °C at a heating rate of 20 °C/min with sample sizes of $10\pm1$ mg in an no lid aluminum sample cup at a 150 ml/min gas flow. Thermal stability was evaluated by determining for each sample the initial degradation temperature corresponding at 5% weight loss ($T_{5\%}$), the weight ($W_i$) and corresponding temperature ($T_{max},i$) at the maximum weight loss rate of each degradation step ($i$) and the percentage of the char residue at a temperature of 700 °C. A Bruker Tensor 27 FTIR spectrometer was coupled with the TGA apparatus to analyze the gaseous emission released real time during each TGA test. Each infrared spectrum was recorded in a wavenumber range of 4000–740 cm$^{-1}$ using 1.0 cm$^{-1}$ spectral resolution and 64 scans. Results were analyzed using OPUS 8.2 spectroscopy software.

### 2.2.3 Cone calorimeter

Cone calorimeter (CC) tests were performed according to the ISO 5660-1 [24], utilizing a Dark Star Research Ltd (UK) apparatus. The samples sizes were 100 mm x 100 mmx 24 mm and were horizontally placed in a stainless-steel metal holder. The back and sides of the sample were insulated with 2 sheets of 3 mm thick high temperature vitreous wool Insulfrax® Paper having a

nominal density of 150 kg/m$^3$ and conductivity 0.098 W/mK at 400 $^o$C, coated with 0.07 mm AT502 30 Micron aluminum foil tape, Category 1 according to BS476 Part 6 and 7 [25, 26]. All samples were conditioned before testing according to ISO 554 [27] at 23$^o$C+/-2 $^o$C at 50 % +/- 5 % relative humidity. The tests were repeated at least twice for each formulation to check reproducibility. To avoid preheating effects, the surface of each sample was carefully insulated before exposure to heat. The following parameters were investigated for each sample: time to ignition (TTI); Combustion Time (CT); Total HRR (THR); peak HRR (p-HHR); average HRR (Av-HRR); average mass loss rate (Av-MLR), smoke production rate (SPR); smoke and CO yield. Specimen burning and smoke color observations were recorded by positioning two digital cameras facing and sideways of the test apparatus. Two heat flux levels were used to examine the fire performance of the samples at both low (20 kW/m$^2$) and high (50 kW/m$^2$) heat fluxes. The uncertainty of the measurements conformed to ISO 5660 [28].

### 2.2.4 Thermal conductivity

Plane Source method was used to measure the sample's thermal conductivity in accordance to ISO 22007-2 [29] at 10 $^o$C was reduced from 31.5 mW/mK for neat PIR to 25.6 mW/mK and 24.8 mW/mK for PLEAPP1 and PLEAPP2 samples respectively, Table 1.

### 3 Results and discussion

### 3.1 Optical Microscopy and FE-SEM

Optical microscopy and FE-SEM, Figures 1 and 2, were used to evaluate the morphology and cellular structure for selected PIR formulations. Figure 1 shows that LDHs do not significantly alter the morphology of the PIR samples. The FE-SEM results indicate that the average cell diameters of REF, PL, PLE, PLEAPP1 and PLEAPP2 samples are presented in Table 1. A slight decrease in the average cell diameter with fillers addition was observed.

### 3.2 Thermogravimetric analysis and gas phase flame retardancy

Combined FTIR/TGA analysis was used to understand the pyrolysis of the PIR samples by identifying the gases evolved at different stages of their pyrolysis. Figures 3 and 4 present the weight and derived weight loss rate of all samples under $N_2$ and Air atmospheres respectively. A summary of the results is provided in Table 2. TGA analysis revealed that degradation temperature of filler layered PIR samples decreases, when compared to the virgin PIR samples (REF). PIR samples containing APP degrade in two steps, under both inert and reactive atmospheres. Those two steps are associated with the degradation of the hard segment urethane-urea linkages and of the polyol derived products from isocyanurate. During those processes low calorific combustion products are initially released during the first degradation step and later higher calorific combustion products are produced due to the polyol derived products of the second degradation step. With the addition of APP, an additional degradation step was observed at around 530 $^oC$ associated with the degradation of APP. Combination of such phosphorus containing additives, e.g. APP, with LDHs has been shown to improve the additives dispersion within the polymer mix. A major advantage of their combination is also the observed reduction in the overall additive concentration required to achieve satisfactory flame-retardant properties in thermoplastics [30]. The initial degradation temperature, $T_{5\%}$, is 258 $^oC$ for pure PIR. $T_{5\%}$ decreases slightly with the addition of LDH compared to neat PIR foam, whereas much more substantially EG-containing formulations (w/wo APP). The first pyrolysis step observed in between 200 $^oC$ and 400 $^oC$, is identified as the primary mass loss step [31, 32].

The temperature at the maximum degradation rate, $T_{max,1}$, is slightly decreased with the LDH filler, whereas it is substantially decreased with the incorporation of EG or EG with APP. This behaviour is owed to the degradation of the hard segment [33] and the residual weight of this first reaction is denoted as $W_1$. The degradation of the polyol derived products, second decomposition stage, resulted in lower residual weight denoted as $W_2$ and was observed between 400 $^oC$ and 600 $^oC$. Maximum degradation temperature during this step, $T_{max,2}$, is 457 $^oC$ and residue mass, 25.4 % were observed for PIR samples under air atmosphere. EG addition resulted in $T_{max,2}$ and mass residue decrease due to fillers degradation at lower temperatures. The former decrease is more substantial with the addition of EG and APP [13, 14, 15]. It is also important to note that the final residue of APP containing formulations is significantly higher than that of other formulations,

indicating that APP is a very effective charring agent. Results are in line with earlier findings from the literature [30, 34, 35] indicating that APP additives decompose at elevated temperatures and produce phosphoric and polyphosphoric acids. Those acids are known to promote charring via formation of reactive polymer fragments cross-linkages that prevent or slow down heat transfer. Oxygen and combustible volatiles cannot easily transfer into the pyrolysis zone due the formation of this carbonized char network. The combination of EG, LDH and APP results in a third degradation step after 500 °C. Addition of EG and LDH with APP serves to reduce depolymerization and enhanced char formation perhaps due to synergistic interactions [30]. For samples PLEAPP1 and PLEAPP2 the final residue is about 37 % in both atmospheres.

Gaseous emissions FTIR spectrums are displayed in Figure 5 for all samples in both atmospheres and at various temperatures. The characteristic bands of degradation of pure PIR can be identified as hydrocarbons (3000-2850 $cm^{-1}$), aromatic compounds (1638 $cm^{-1}$), $CO_2$ (2400-2300 $cm^{-1}$), -NCO compounds (2300-2200 $cm^{-1}$), CO (2181 $cm^{-1}$) and ethers (1153 $cm^{-1}$). The degradation of the polymer polyol and urethane is visible in the changes of the spectra between 1000-1500 $cm^{-1}$ wavelengths, clearer under $N_2$ atmosphere, consistent to the literature [33]. PIR samples containing EG, APP1 And APP2 release similar pyrolysis products to pure PIR samples.

Utilising the FTIR spectra, we performed integration over specific wavenumber ranges and determine the absorbance intensity of the different pyrolysis gases. Figure 6 demonstrates a comparison of the absorbance of ethers, -NCO, CO and $CO_2$ over time for all samples in air. CO was detected between 200 °C and 650 °C with a maximum value at 500 °C, under air atmosphere and from 100 °C to 1000 °C with a second maximum value at 950 °C for samples containing APP1 and APP2 under inert atmosphere. Carbon dioxide emissions show one peak between 350 °C and 700 °C with a maximal value at 600 °C under inert atmosphere. Two peaks are observed under air atmosphere and the maximal values are recorded at a lower temperature of 500 °C. Gaseous emissions pattern detected in this work are consistent with previous results [5-7, 36] regarding the thermal degradation and carbonization performance of PIR with different fire-retardant fillers.

### 3.3 Cone calorimetry

HRR and SPR histories of all formulations at 20 kW/m$^2$ and 50 kW/m$^2$ are depicted in Figures 7 and 8. It is worth noting that all formulations (except PLEAPP1 at 20 kW/m$^2$) ignited almost immediately after being exposed to the heat source, due to their low density and high flammability. Neat PIR has the highest HRR and SPR as expected. Fissures were observed on the final char residue at the end of the test along with detachment and exfoliation of the upper layer surface as highlighted in Table 3. The trends of SPR are similar to those of HRR, and consequently we will focus our discussions on the HRR. With the addition of LDH alone, there is a small decrease in the first HRR peak with a more substantial reduction in the second HRR peak. The char also appears stronger than that of the neat PIR. APP addition to PIR samples resulted in lower PHRR values or no ignition at the lower heat flux. Simultaneous presence of LDH and APP in PIR samples can successfully promote char formation. This concurs well with previous research on chemical interaction of APP and LDH in polystyrene [30]. With a further inclusion of EG, the HRR is reduced further, however, it is interesting to note that APP2 has limited effect on the HRR compared to EG alone, whereas PLEAPP1 achieves the lowest HRR and SPR, most likely because of the increased strength of the char layer as shown in Table 3. This strengthened char layer provides a resilient barrier, preventing heat and oxygen penetration to the material and release of non-combustible gases. At the same time, it can effectively suppress smoke and gases during the combustion process. The present results demonstrate that the degree of polymerization has a very important effect on the fire retardancy of the composites as shown in both Figures 7, 8 and Table 3.

Another important finding is that LDH decreases smoke and CO yields compared to neat PIR (REF). Improved fire behaviour when EG and APP2 fillers are used, is evident as the flame-retardant properties of PLEAPP2 sample are improved significantly. Both the p-HRR and Av-HOC are decreased with additions of fillers. EG having considerably lower values of heat of combustion than REF or PL confirms that it also acts in the gaseous phase in suppressing combustion [17]. One other important observation is that all the fillers have either similar or lower smoke or CO yields compared to neat PIR, highlighting one of their main advantages of these type of fire retardants in comparison to halogenated fire retardants.

### 3.4　SEM and Raman residual char characterization

Figure 9 presents the char residue of all samples after CC testing under both heat fluxes. Fillers were found to promote the formation of more rigid and hardened residual char layer. In virgin PIR samples, the char was brittle and non-uniformly distributed. In addition, detachment and exfoliation of the upper layer surface was also observed. A clear difference in appearance was observed in the residual char for PLEAPP1 and PLEAPP2, which were intact and spongy. Clearly, the strength and integrity of the char plays a very important role in reducing the burning rate/heat release rate for meso- to large-scale samples, in which internal heat and mass transfer becomes important, as opposed to the mg samples used in TGA. Plain PIR char residues show a looser structure, which indicates inefficient barrier protection for underlying layers. PL char residue was more coherent. The addition of EG resulted in a more compact char structure although minor cracks in the surface could still be observed. Comparing to the rest of the char residue morphologies, the char residues PLEAPP1 samples were more compact than the rest of the samples and no cracks appeared on the surface.

Char residues were further evaluated in terms of field mission SEM analysis to explore the specific mechanisms. Char samples investigated were taken after performing CC at high heat flux of 50 kW/m$^2$. In Figure 10 (a)-(c), it can be observed that cells were severely broken, and an open cell polyhedral structure was dominant in virgin PIR samples. With the addition of 2 % LDH, Figure 10 (d)-(f), PL sample's cellular structure became loose and permeable and this was an indication that the flame shield created was not as strong. Numerous bright amorphous regions scattered across the image are identified as residual fillers. In the rest of the samples containing EG, Figure 10 (g)-(h), (j)-(k), (m)-(n), "worm-like" char regions are observed and scattered throughout their porous sheeted structure as also reported in [37]. The addition of APP1 and APP2 results in a tighter and denser morphology than the materials added with only expandable graphite, in accordance to previous studies [38]. The fact that the combination of APP, EG and LDH can promote the formation of an intumescent residue with superior barrier properties compared to samples containing only APP is likely due to the combination of a reduced heat and mass transfer due to intumescence and reduced permeability of the residue [30].

The graphitic structure of PLE, PLEAPP1 and PLEAPP2 char residue samples was investigated with Raman spectroscopy, Figure 11. The G peak at 1580 $cm^{-1}$ corresponds to vibrations of in plane $sp^2$ carbon atoms in graphite. The D peak at 1350 $cm^{-1}$ is associated with the vibration of carbon atoms in disordered graphitic structures [38]. The graphitized structure, acts as a physical barrier and is an indication of increased thermal stability. D and G intensity band ratio ($I_D/I_G$) was utilized for estimating the degree of graphitization in residual char; a higher degree of graphitization is associated with decreased $I_D/I_G$ values [39]. PLE sample exhibited the lowest $I_D/I_G$ value of 0.12, hence the highest degree of graphitization, followed by samples PLEAPP1 and PLEAPP2, which exhibited values of 0.40 and 0.48 respectively.

## 4    Flame retardant mechanism of LDH, EG and APP additives on flame retardancy

Figure 12 represents the proposed mechanism of LDH, EG and APP additives on flame retardancy of PIR. APP, EG and LDH can promote the formation of an intumescent residue with superior barrier properties [10, 12, 13, 14, 15, 17]. It is attributed to the combination of a reduced mass and heat transfer mechanism, due to reduced permeability residue and intumescent [12].

As it is depicted, the existence of a resilient char layer is crucial for guarantying the flame retardancy of the underlying PIR matrix. Cone calorimetry and thermogravimetric analysis revealed that a strong char layer can prevent penetration of heat and oxygen and thus reducing PIR thermal degradation, decreasing HRR and pyrolysis gas release. Formation of a resilient char layer also shields the rest of the sample underneath it from radiation. The diffusive gases navigate around LDH and APP nanofillers that act as barriers preventing pyrolysis gases to move towards the exposed surface. APP was found to act in the condensed phase and acts in a beneficial way as it promotes sample dehydration and carbon-forming.

During thermal decomposition, LDH fillers lose the interlayer water. The decomposition of the intercalated anions and metal hydroxide produces water vapor and gases, e.g. $CO_2$, which eventually reduce the availability of combustible fuel vapors resulting in decreased heat release and promotion of char formation.

Cone calorimetry revealed that smoke and CO yields values of all formulations containing LDH, APP and EG are similar, lower than those of virgin PIR. This is a strong indication that neither of the fillers promote pyrolysis gases production. It can also be speculated that the samples containing APP were more cohesive and formed more compact char layer. Intumescence of the char in PLEAPP1 and PLEAPP2 samples is stabilized and improved as the right proportion of LDH crosslink with APP; further to that, they present increased viscosity due to higher molecular weight APP and the presence of EG. The fact that samples containing EG have considerably lower values of heat of combustion than REF or PL samples confirms that EG also acts in the gaseous phase in accordance to bibliography [17].

## 5    Conclusions

Fire-reaction properties and thermal stability of PIR form with smart fillers including LDHs, EG and APPs were evaluated using thermogravimetry and cone calorimetry. Optical microscopy and scanning electron microscopy measurements were also performed for the samples, which verified that the fillers were exfoliated in the PIR samples. Post-burning characterization and morphological assessment of the residual materials revealed that all fillers stimulate the formation of a reinforced char layer. LDHs alone have limited effect on reducing the HRR or SPR since they only act in the solid phase. With the addition of EG or EG+APP, the HRR is further decreased owing to the increased char strength as well as the release of non-combustible gases that during combustion adequately suppress smoke and gases production. There are strong indications that additives studied in this work can effectively slow down or even prevent depolymerization of PIR and simultaneously promote char formation. The best performance was achieved by PLEAPP1 with high degree of polymerization that resulted in resilient char formation, decreased heat release values, smoke generation and CO production. This result confirms that the degree of polymerization of fire retardants is significant in its fire performance.

The present results clearly indicate that the use of smart fillers (LDH, EG and APP) in PIR foams can significantly increase their thermal stability and fire behaviour, which is of great importance in the development of safe and highly efficient insulation products that can be used in the building industry, and especially in cost-effective building envelopes in order to bring opaque components

of curtain wall building systems to "nearly zero energy" standards. Whilst we used only small-scale samples in this work, it is worth noting that preliminary tests of selected formulations in single-burning-item (SBI) have been carried out with promising results. Further assessment of the fire performance of the foams incorporated into a complete façade system will also be conducted in furnace tests in the near future.

Credit author statement

**Eleni ASIMAKOPOULOU:** Conceptualization, methodology, investigation, formal analysis, validation, writing-original draft. **Jianping ZHANG**: Conceptualization, methodology, validation, writing-review and editing. **Maurice McKEE:** investigation. **Kinga WIECZOREK:** resources, methodology. **Anna KRAWCZYK:** resources, methodology, validation, wirting-review and editing. **Michele ANDOLFO**: resources, methodology. **TomaszKOZLECKI:** resources, methodology, validation, wirting-review and editing. **Marco SCATTO:** resources, methodology. **Michele SISANI:** resources, methodology. **Maria BASTIANINI:** resources, methodology. **Anastasios KARAKASSIDES:** methodology, validation, wirting-review and editing. **Pagona PAPAKONSTANTINOU:** methodology, validation, wirting-review and editing.

## Declaration of interests

☒ The authors declare that they have no known competing financial interests or personal relationships that could have appeared to influence the work reported in this paper.

## 6    Acknowledgements

**References**

[1] UN Environment and International Energy Agency 2017: Towards a zero-emission, efficient, and resilient buildings and construction sector. Global Status Report 2017.

[2] Directive 2018/844/EU of the European Parliament and of the Council of 30 May 2018 amending Directive 2010/31/EU on the energy performance of buildings and Directive 2012/27/Eu on energy efficiency. Off. J. Eur. Union 2018, 156, 75–91.

[3] D. O'Connor, The Building Envelope: Fire Spread, Construction Features and Loss Examples, SFPE Handbook of Fire Protection Engineering (5th ed) Hurley M.J. (ed.), National Fire Protection Association, Quincy, MA 02269, 2016, p 3242/3512.

[4] Y.C. Li, Y.H. Yang, J.R. Shields, R.D. Davis, Layered double hydroxide-based fire-resistant coatings for flexible polyurethane foam, Polymer 56 (2015) 284-292, https://doi.org/10.1016/j.polymer.2014.11.023

[5] S. Gomez-Fernandez, L. Ugarte, C. Pena-Rodriguez, M. Zubitur, M.A. Corceuera, A. Eceiza, Flexible polyurethane foam nanocomposites with modified layered hydroxides, Appl. Clay Sci. 123 (2016) 109-120, https://doi.org/10.1016/j.clay.2016.01.015

[6] K. Chen, C. Tian, S. Liang, X. Zhao, X. Wang, Effect of stoichiometry on the thermal stability and flame retardation of polyisocyanurate foams modified with epoxy resin, Polym. Degrad. Stabil. 150 (2018) 105-113, https://doi.org/10.1016/j.polymdegradstab.2018.02.015

[7] M. Kuranska, U. Cabulis, M. Auguscik, A. Prociak, J. Ryszkowaska, M. Kirpluks, Bio-based polyurethane-polyisocyanurate composites with an intumescent flame retardant, Polym. Degrad. Stabil. 127 (2016) 11-19, https://doi.org/10.1016/j.polymdegradstab.2016.02.005

[8] D.Y. Wang, Novel fire-retardant polymers and composite materials (1st ed) Woodhead Publishing Series in Composite Science and Engineering, Woodhead Publishing, 2016.

[9] E. Asimakopoulou, J. Zhang, M. McKee, K. Wieczorek, A. Krawczyk, M. Andolfo, M. Scatto, M. Sisani, M. Bastianini, A. Karakassides, P. Papakonstantinou, Fire Retardant Action of Layered Double Hydroxides and Zirconium Phosphate Nanocomposites Fillers in Polyisocyanurate Foams. Fire Technol. (2020), https://doi.org/10.1007/s10694-020-00953-7

[10] Asimakopoulou E., Zhang J., McKee M., Wieczorek K., Krawczyk A., Andolfo M., Scatto M., Michele S., Bastianini M., Assessment of fire behaviour of polyisocyanurate (PIR) insulation foam enhanced with lamellar inorganic smart fillers, IOP Conf Series: Journal of Physics: Conf Series 1107: 032004 (2018), https://doi:10.1088/1742-6596/1107/3/032004

[11] L. Gao, G. Zheng, Y. Zhou, L. Hu, G. Feng, M. Zhang, Synergistic effect of expandable graphite, diethyl ethylphosphonate and organically-modified layered double hydroxide on flame retardancy and fire behavior of polyisocyanurate-polyurethane foam nanocomposite, Polym. Degrad. Stabil. 101 (2014) 92-101, https://doi.org/10.1016/j.polymdegradstab.2013.12.025

[12] Y. Liu, Y. Gao, Q. Wang, W. Li n, The synergistic effect of layered double hydroxides with other flame-retardant additives for polymer nanocomposites: a critical review, Dalton Trans. 47 (2018) 14827-14840, https://doi.org/10.1039/c8dt02949k

[13] C. X. Zhao, Y. Liu, D. Y. Wang, D. L. Wang and Y. Z. Wang, Synergistic effect of ammonium polyphosphate and layered double hydroxide on flame retardant properties of poly(vinyl alcohol), Polym. Degrad. Stab. 93 (2008) 1323-1331, https://doi.org/10.1016/j.polymdegradstab.2008.04.002

[14] C. X. Zhao, G. Peng, B. L. Liu and Z. W. Jiang, Synergistic effect of organically modified layered double hydroxide on thermal and flame-retardant properties of poly(butyl acry-late-vinyl acetate), J. Polym. Res. 18 (2011) 1971–1981, https://doi.org/10.1007/s10965-011-9604-8

[15] P. Ding, S. F. Tang, H. Yang and L. Y. Shi, PP/LDH nano-composites via melt-intercalation: synergistic flame retard-ant effects, properties and applications in automobile industries, Adv. Mater. Res. 87–88 (2009) 427–432, https://doi.org/10.4028/www.scientific.net/AMR.87-88.427

[16] L. C. Du, Y. C. Zhang, X. Y. Yuan and J. Y. Chen, Combustion characteristics and synergistic effect of halogen-free flame-retarded EVA/hydrotalcite blends with expandable graphite and fumed silica, Polym. Plast. Technol. Eng. 48 (2009) 1002–1007, https://doi.org/10.1080/0360255090 3092500

[17] X. Y. Pang, Y. Tian and X. Z. Shi, Synergism between hydro-talcite and silicate-modified expandable graphite on ethylene vinyl acetate copolymer combustion behavior, J. Appl. Polym. Sci. 134 (2017) 44634, https://doi.org/10.1002/app.44634

[18] X.M. Hu, D.M. Wang, Enhanced fire behavior of rigid polyurethane foam by intumescent flame retardants, J. Appl. Polym. Sci. 129 (2013) 238-246, https://doi.org/10.1002/app.38722

[19] X. Meng, L. Ye, X. Zhang, P. Tang, J. Tang, X. Ji, Z. Li, Effects of expandable graphite and ammonium polyphosphate on the flame retardant and mechanical properties of rigid polyurethane foams, J. Appl. Polym. Sc. 114 (2009) 853-863, https://doi.org/10.1002/app.30485

[20] M. Kirpluks, U. Cabulis, V. Zeltins, L. Stienra, A. Avots, Rigid polyurethane foam thermal insulation protected with mineral intumescent mat, Autex Research Journal 14 (2014) 259-269, https://doi.org/10.2478/aut-2014-0026

[21] M. Modesti, A. Lorenzetti, Flame retardancy of polyisocyanurate–polyurethane foams: use of different charring agents, Polym. Degrad. Stabil. 78 (2002) 341-347, https://doi.org/10.1016/S0141-3910(02)00184-2

[22] G. Camino, S. Duquesne, R. Delobel, B. Eling, C. Lindsay, T. Roels, In: G.L. Nelson, C.A. Wilkie, editors. Symposium Series No797/ Fires and Polymers. Materials and Solutions for Hazard Prevention. Washington DC: ACS Pub., 2001, p 90/109.

[23] M. Thirumal, D. Khastgir, N. K. Singha, B. S. Manjunath, Y. P. Naik, Effect of Expandable Graphite on the properties of intumescent flame-retardant polyurethane foam, J. Appl. Polym. Sci. 108 (2008) 2586, https://doi.org/10.1002/app.28763

[24] ISO 5660-1, Reaction to fire tests – Heat release, smoke production and mass loss rate – Part 1: Heat release rate (cone calorimeter method), International Organization for Standardization, Geneva, Switzerland, 2002.

[25] British Standards Institution (1989) 476-6: Fire tests on building materials and structures - Method of test for fire propagation for products.

[26] British Standards Institution (1997) 476-7: Fire Tests on Building Materials and Structures - Method of test to determine the classification of the surface spread of flame of products.

[27] ISO 554, Standard atmospheres for conditioning and/or testing specifications, International Organization for Standardization, Geneva, Switzerland, 1974.

[28] ISO 5660-1 (2002) Reaction to fire tests – Heat release, smoke production and mass loss rate – Part 1: Heat release rate (cone calorimeter method), International Organization for Standardization, Geneva, Switzerland.

[29] ISO 22007-2 (2015) Plastics – Determination of thermal conductivity and thermal diffusivity – Part 2: Transient plane heat source (hot disk) method, International Organization for Standardization, Geneva, Switzerland.

[30] C. Nyambo, E. Kandare, D. Wang, C. Wilkie, Flame-retarder polystyrene: Investigating chemical interactions between ammonium polyphosphate and MgAl layered double hydroxide, Polym, Degrad. Stab. 93 (2008) 1656-1663, https://doi.org/10.1016/j.polymdegradstab.2008.05.029

[31] J.O. Hidalgo, J.L. Torero, S. Welch, Experimental characterization of the fire behaviour of thermal insulation materials for a performance-based design methodology, Fire Technol. (2017) 1201-1232, https://doi.org/10.1007/s10694-016-0625-z

[32] D.K. Chattopadyay, D.C. Webster, Thermal stability and flame retardancy of polyurethanes, Progr. Polym. Sci. (2009) 1008-1133, https://doi.org/10.1016/j.progpolymsci.2009.06.002

[33] L. Jial, H. Xiao, Q. Wang, J. Sun, Thermal degradation characteristics of rigid polyurethane foam and volatile products analysis with TG-FTIR-MS, Polym, Degrad. Stab. 98 (2013) 2687-2696, https://doi.org/10.1016/j.polymdegradstab.2013.09.032

[34] B. K. Kandola, R. A. Horrocks, P. Myler, D. Blair, New developments in flame retardancy of glass-reinforced epoxy composites, J. Appl. Polym. Sci. 88 (2003) 2511–21, https://doi.org/10.1002/app.11909

[35] B. K. Kandola, S. Horrocks, R. A. Horrocks, Evidence of interaction in flame-retardant fibre-intumescent combinations by thermal analytical techniques, Thermochim. Acta 294 (1997)113–25, https://doi.org/10.1016/S0040-6031(96)03151-6

[36] J. Xu, T. Wu, C. Peng, S. Adegbite, Influence of acid and alkali pre-treatments on thermal degradation behaviour of polyisocyanurate foam and its carbon morphology, Polym. Degrad. Stabil. 141 (2017) 104-118, https://doi.org/10.1016/j.polymdegradstab.2017.05.018

[37] X. Shi, S. Jiang, J. Zhu, G. Li, X. Peng, Establishment of a highly efficient flame-retardant system for rigid polyurethane foams based on bi-phase flame-retardant actions, RCS Adv., 8 (2018) 9985-9995, https://doi.org/10.1039/C7RA13315D

[38] K.S. Lim, S.T. Bee, L.T. Sin, T.T. Tee, C.T. Ratnam, D. Hui, A.R. Rahmat, A. R., A review of application of ammonium polyphosphate as intumescent flame retardant in thermoplastic composites, Compos. Part B-Eng. 84 (2016) 155-174, https://doi.org/10.1016/j.compositesb.2015.08.066

[39] F. Tuinstra and J. L. Koenig., Raman Spectrum of Graphite, J. Chem. Phys. 53 (1970) 1126-1130, https://doi.org/10.1063/1.1674108
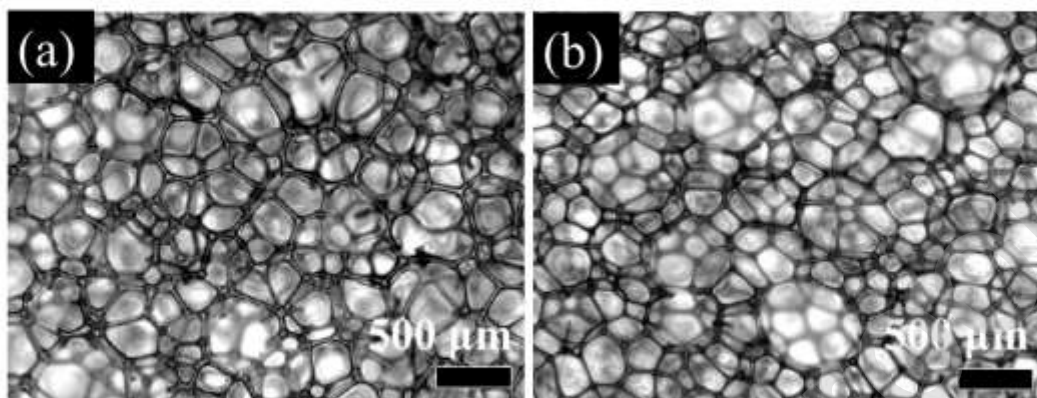
**FIGURE CAPTIONS**



Figure 1: Morphological evaluation using optical microscopy (500 μm scale) of REF (a) and Pl (b) samples.
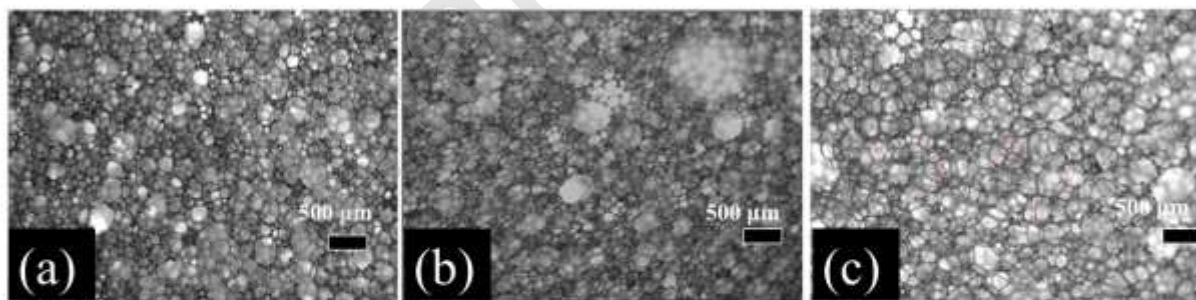


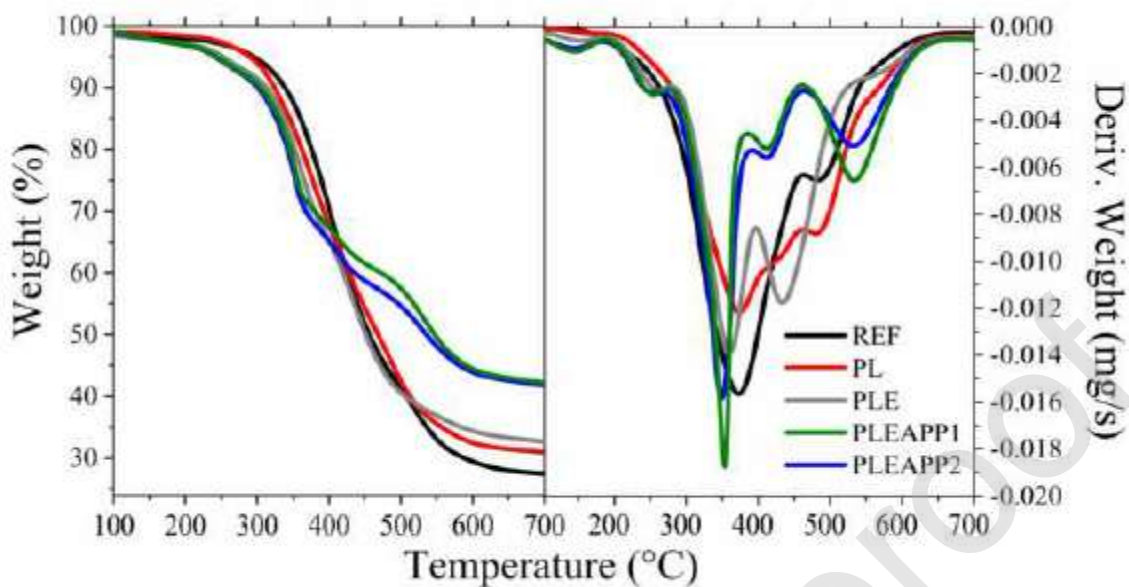Figure 2: SEM images (500 μm scale) of PLE (a), PLEAPP1 (b), PLEAPP2 (c) samples.

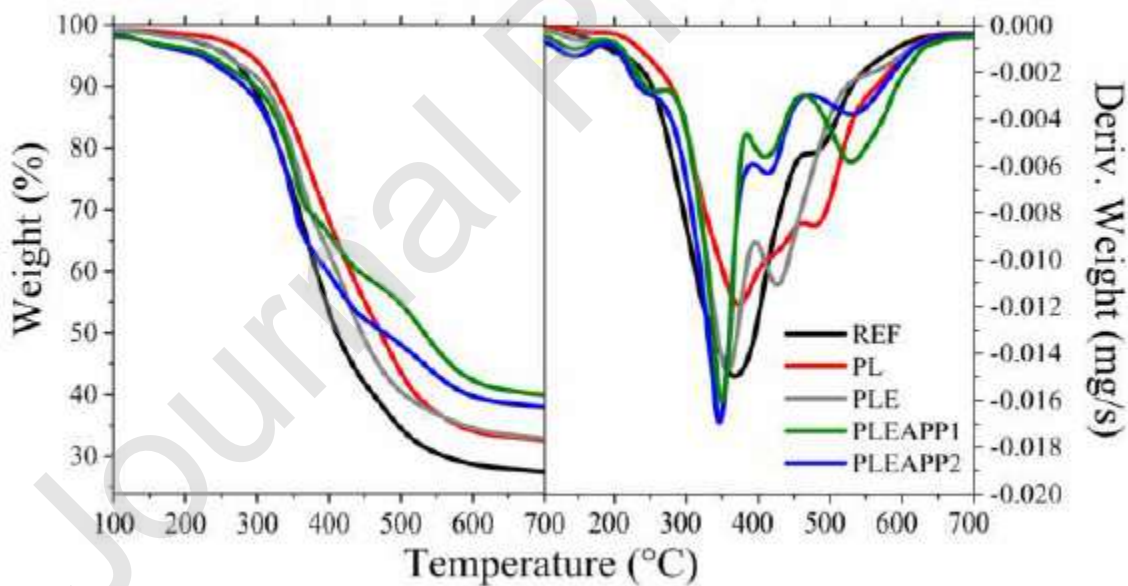Figure 3: TGA (left) and DTGA (right) of all the formulations in $N_2$ atmosphere.



Figure 4: TGA (left) and DTGA (right) of all the formulations in air atmosphere.
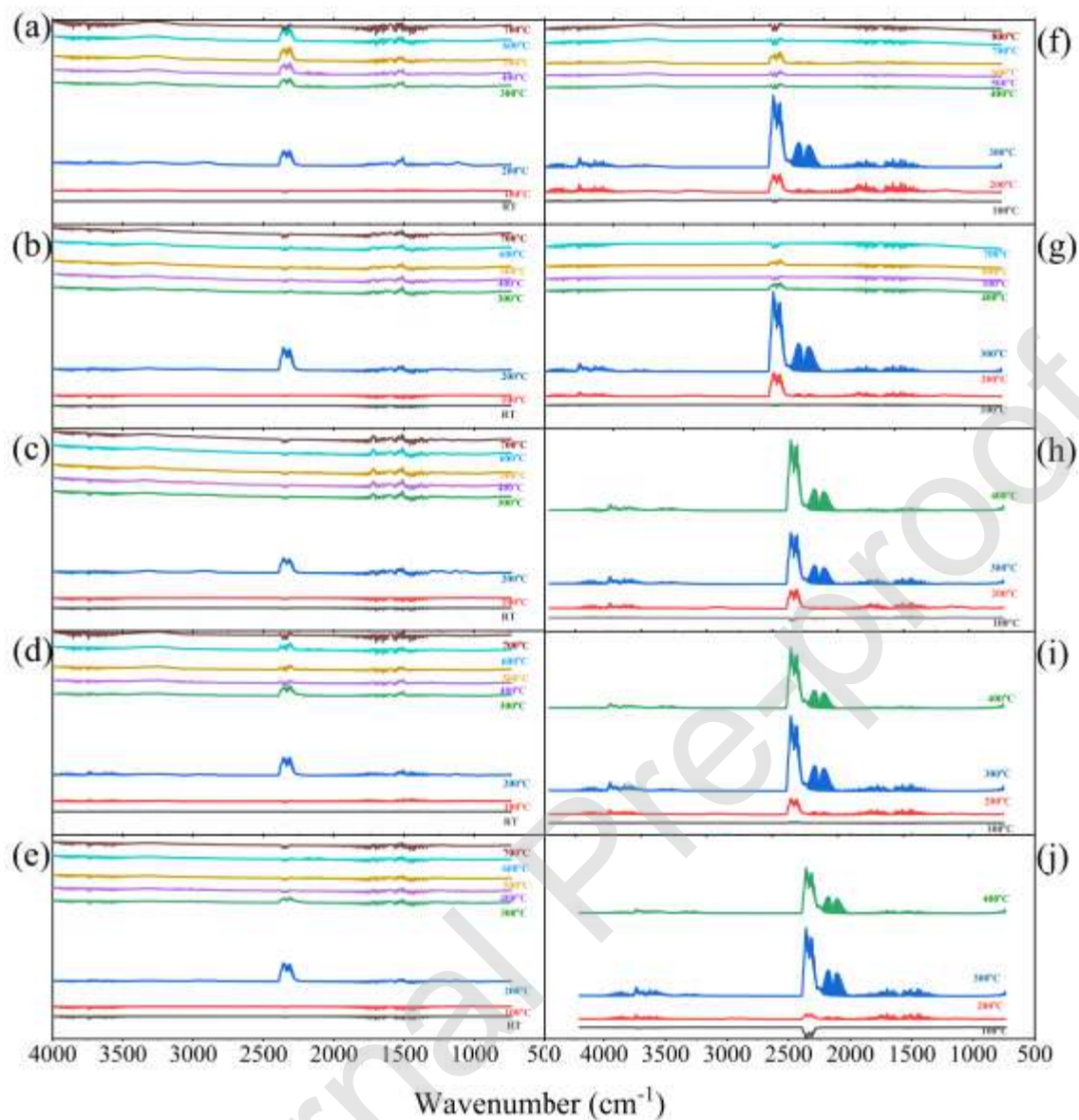
Figure 5: Real time FTIR spectra of (a) and (f) REF, (b) and (g) PL, (c) and (h) PLE, (d) and (i) PLEAPP1, (e) and (j) PLEAPP2 samples, in $N_2$ (a)-(e), and air, (f)-(j) atmosphere.
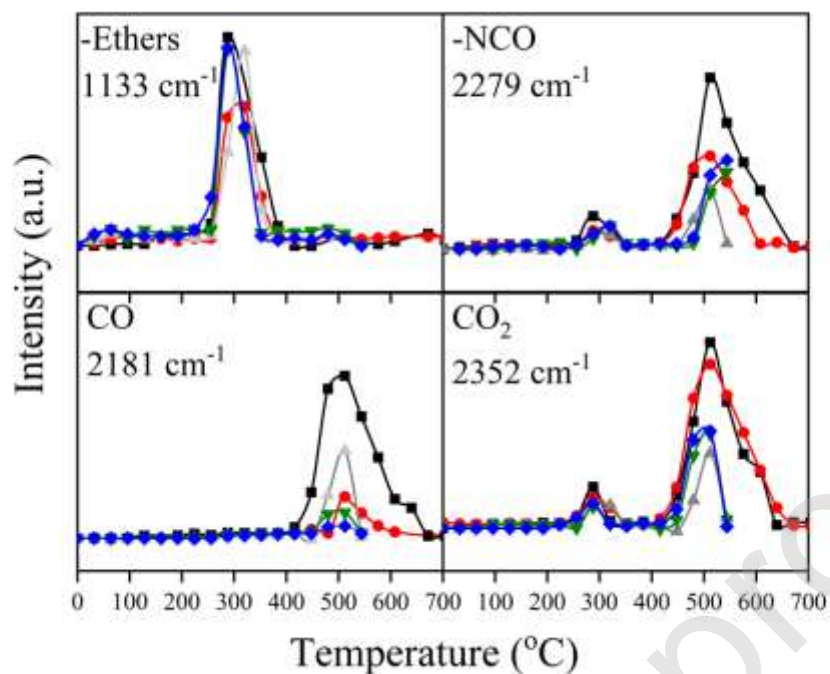
Figure 6: Temporal absorbance of pyrolysis products of all samples: (a) ethers (1133 cm$^{-1}$), (b) NCO (2279 cm$^{-1}$), (c) CO (2181 cm$^{-1}$), (d) $CO_2$ (2352 cm$^{-1}$) samples under air atmosphere.
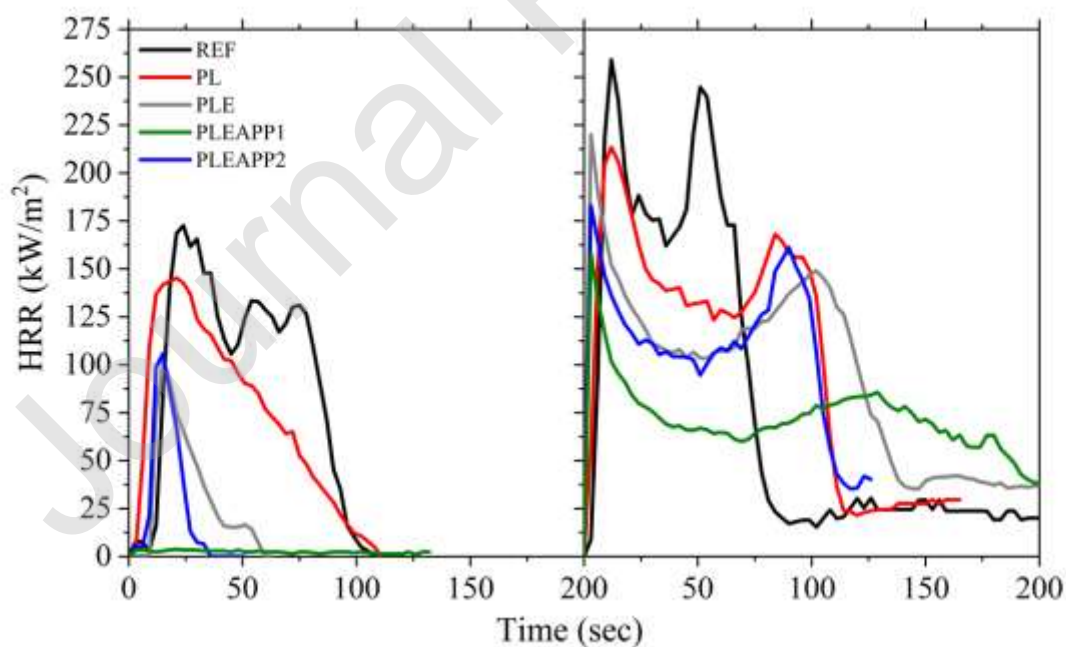


Figure 7: Comparisons of HRR at 20 kW/m$^2$ (left) and 50 kW/m$^2$ (right) of all formulations.
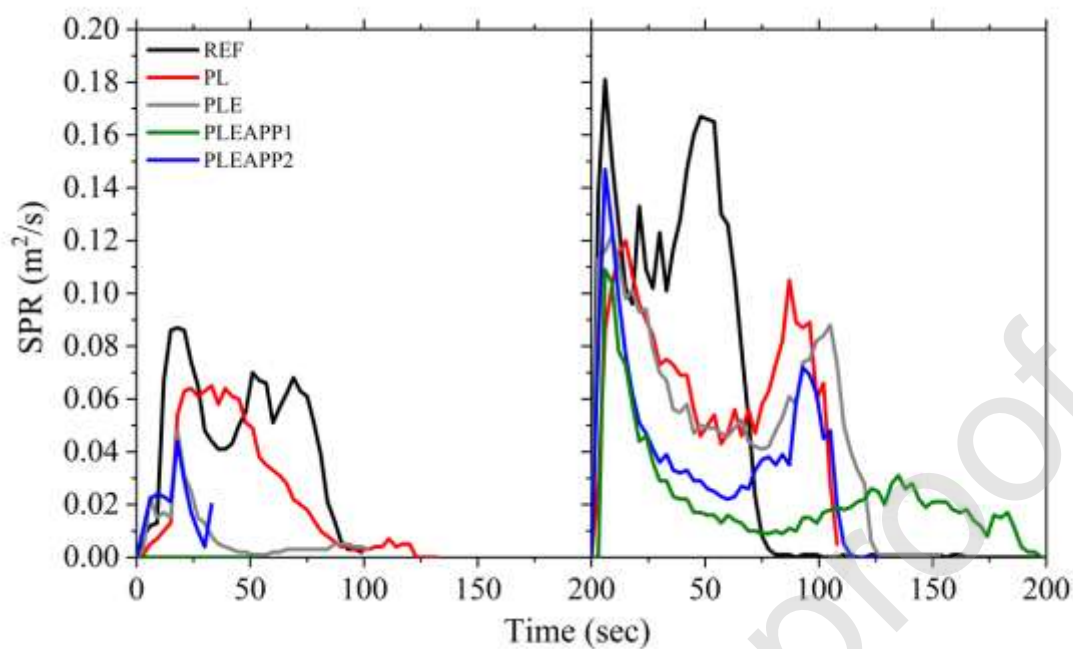
Figure 8: Comparisons of SPR at 20 kW/m$^2$ (left) and 50 kW/m$^2$ (right) of all formulations.
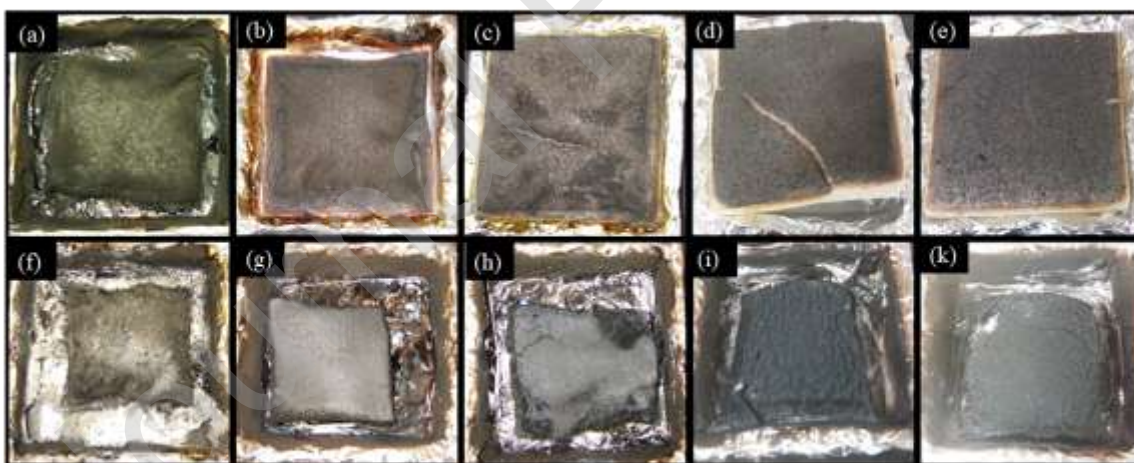
Figure 9: Digital photos of charred samples of (a) and (f) REF, (b) and (g) PL, (c) and (h) PLE, (d) and (i) PLEAPP1, (e) and (j) PLEAPP2 after CC testing at 20 kW/m$^2$, (a)-(e), and 50 kW/m$^2$, (f)-(j).
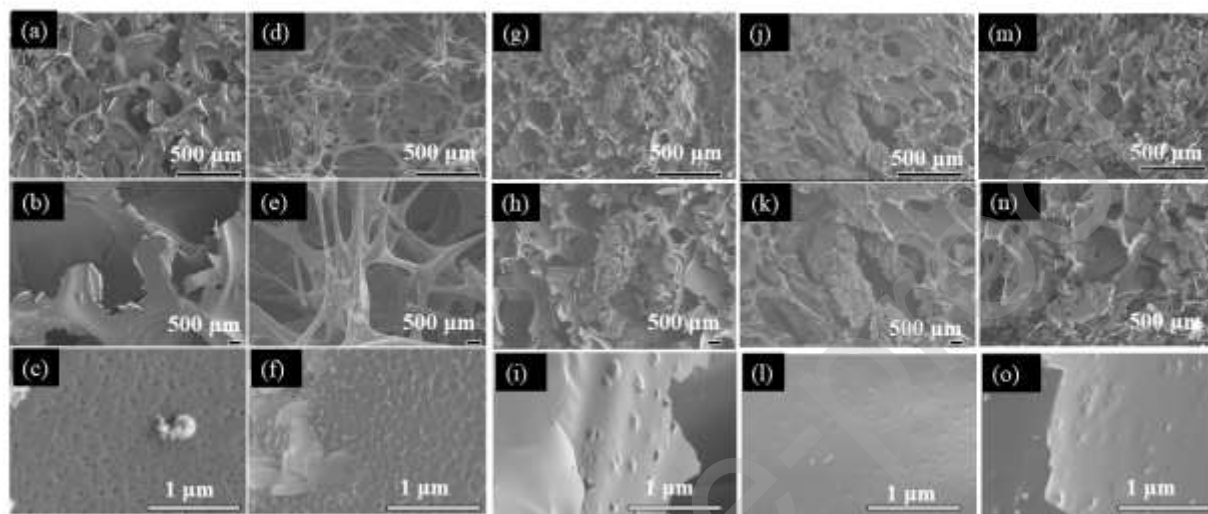


Figure 10: SEM images of (a)-(c) REF, (d)-(f) PL, (g)-(i) PLE, (j)-(l) PLEAPP1 and (m)-(o) PLEAPP2 charred samples.
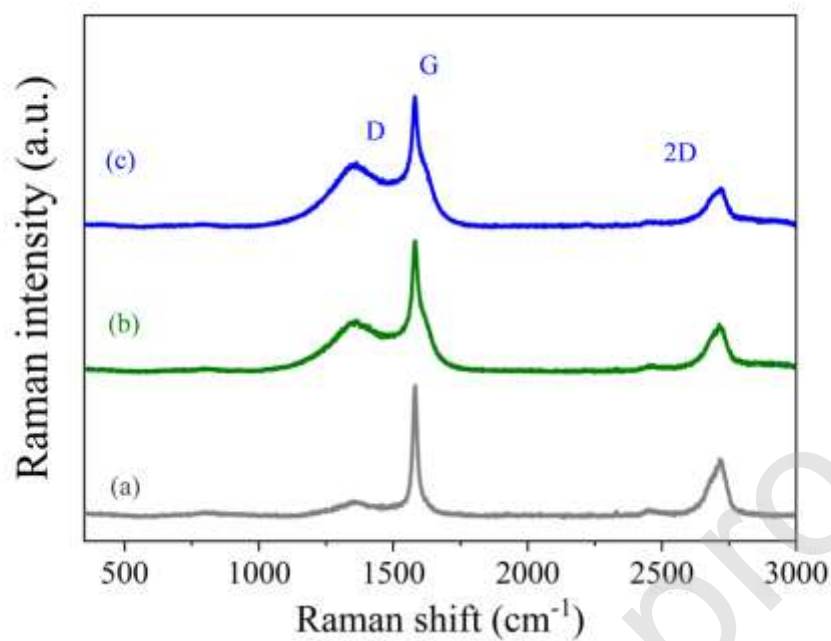
Figure 11: Raman spectra for a) PLE, b) PLEAPP1 and c) PLEAPP2 samples. D, G and 2D represent the characteristic bands of expandable graphite.
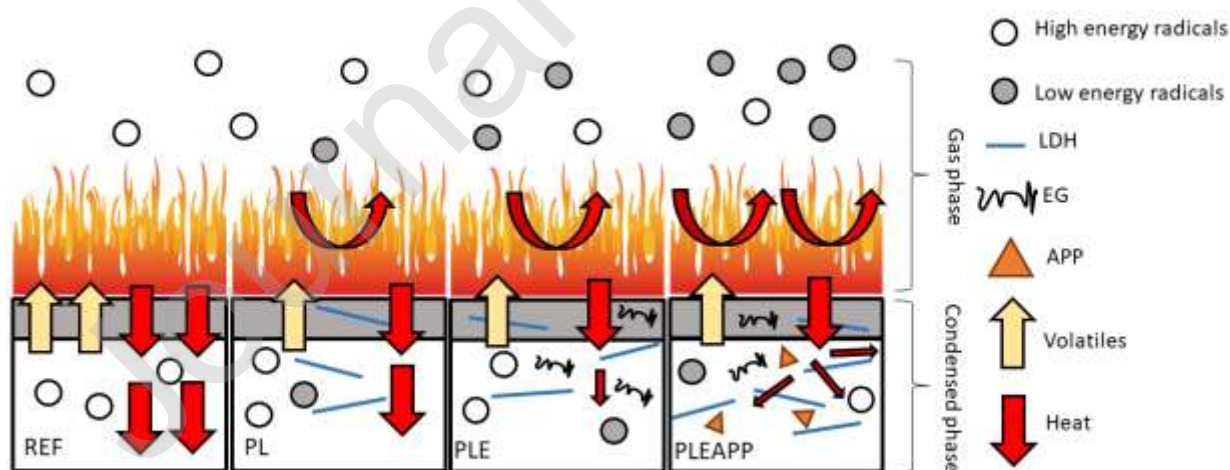
Figure 12: Diagrammatic illustration of the flame-retardant mechanism of LDH, EG and APP additives in PIR samples.

**TABLES CAPTIONS**

Table 1. Samples composition, physical and mechanical characteristics.

| Samples | MgAlCO₃ [% wt] | EG [% wt] | APP1 [% wt] | APP1 [% wt] | Density [kg/m³] | Cell diam. [μm] | Closed cells [%] | Th. Cond. [mW/mK] | Compr. Str. [MPa] | Tensile Str. [kPa] |
|---|---|---|---|---|---|---|---|---|---|---|
| REF | - | - | - | - | 50 | 390 | 97 | 31.5 | <0.30 | - |
| PL | 2 | - | - | - | 43 | 312 | 88 | 28.2 | <0.64 | < 160 |
| PLE | 2 | 5.1 | - | - | 40 | 192 | 90 | 24.0 | <0.78 | < 165 |
| PLEAPP1 | 2 | 5.1 | 3.6 | - | 45 | 142 | 85 | 25.6 | <0.78 | < 165 |
| PLEAPP2 | 2 | 5.1 | - | 3.6 | 45 | 271 | 87 | 24.8 | <0.78 | < 165 |

Table 2. TG/DTG results of all formulations.

| Samples | Gas | $T_{5\%}$ [°C] | $T_{max,1}$ [°C] | $W_1$ [%] | $T_{max,2}$ [°C] | $W_2$ [%] | $T_{max,3}$ [°C] | $W_3$ [%] | Residue 700°C [%] |
|---|---|---|---|---|---|---|---|---|---|
| REF | | 295 | 373 | 80.8 | 480 | 44.7 | - | - | 25.9 |
| PL | | 289 | 374 | 76.0 | 511 | 40.3 | - | - | 28.7 |
| PLE | N₂ | 251 | 360 | 76.9 | 416 | 61.1 | - | - | 30.3 |
| PLEAPP1 | | 241 | 349 | 78.5 | 435 | 62.8 | 534 | 52.2 | 38.8 |
| PLEAPP2 | | 241 | 349 | 77.0 | 425 | 61.3 | 534 | 50.2 | 38.2 |
| REF | | 258 | 372 | 64.1 | 457 | 40.7 | - | - | 25.4 |
| PL | | 290 | 370 | 77.5 | 446 | 55.9 | - | - | 30.3 |
| PLE | Air | 255 | 357 | 76.4 | 429 | 54.7 | - | - | 30.7 |
| PLEAPP1 | | 219 | 349 | 71.8 | 421 | 62.6 | 538 | 49.1 | 37.2 |

| PLEAPP2 | | 232 | 349 | 77.3 | 416 | 56.9 | 538 | 44.3 | 35.7 |

Table 3. Flammability and smoke emission behavior of pure PIR and PIR-layered filler samples.

| | Samples | THR [MJ/m$^2$] | p-HRR [kW/m$^2$] | Av-HOC [MJ/kg] | Smoke yield [-] | CO yield [-] |
|---|---|---|---|---|---|---|
| 20 | REF | 9.98 | 172.6 | 19.6 | $7.9 \times 10^{-2}$ | $3.4 \times 10^{-2}$ |
| | PL | 8.07 | 145.3 | 17.6 | $6.0 \times 10^{-2}$ | $2.6 \times 10^{-2}$ |
| | PLE | 2.00 | 101.8 | 3.9 | $0.8 \times 10^{-2}$ | $0.9 \times 10^{-2}$ |
| | PLEAPP1 | NI | NI | NI | NI | NI |
| | PLEAPP2 | 1.37 | 105.8 | 1.3 | $0.5 \times 10^{-2}$ | $0.2 \times 10^{-2}$ |
| 50 | REF | 17.85 | 259.1 | 49.7 | $9.8 \times 10^{-2}$ | $11.3 \times 10^{-2}$ |
| | PL | 17.15 | 213.4 | 32.1 | $6.9 \times 10^{-2}$ | $4.0 \times 10^{-2}$ |
| | PLE | 16.76 | 207.5 | 20.9 | $7.3 \times 10^{-2}$ | $3.1 \times 10^{-2}$ |
| | PLEAPP1 | 13.66 | 183.0 | 22.5 | $9.1 \times 10^{-2}$ | $5.5 \times 10^{-2}$ |
| | PLEAPP2 | 15.03 | 157.9 | 23.1 | $4.8 \times 10^{-2}$ | $3.8 \times 10^{-2}$ |